

## Different oscillatory entrainment of cortical networks during motor imagery and neurofeedback in right and left handers



Mathias Vukelić, Paolo Belardinelli, Robert Guggenberger, Vladislav Royter, Alireza Gharabaghi \*

Division of Functional and Restorative Neurosurgery, Tuebingen Neuro Campus, Eberhard Karls University Tuebingen, Germany

### ARTICLE INFO

#### Keywords:

Brain-robot interface  
Brain-computer interface  
Robotic rehabilitation  
Cortical connectivity  
Closed-loop stimulation  
State-dependent stimulation  
Stroke

### ABSTRACT

Volitional modulation and neurofeedback of sensorimotor oscillatory activity is currently being evaluated as a strategy to facilitate motor restoration following stroke. Knowledge on the interplay between this regional brain self-regulation, distributed network entrainment and handedness is, however, limited.

In a randomized cross-over design, twenty-one healthy subjects (twelve right-handers [RH], nine left-handers [LH]) performed kinesthetic motor imagery of left (48 trials) and right finger extension (48 trials). A brain-machine interface turned event-related desynchronization in the beta frequency-band (16–22 Hz) during motor imagery into passive hand opening by a robotic orthosis. Thereby, every participant subsequently activated either the dominant (DH) or non-dominant hemisphere (NDH) to control contralateral hand opening. The task-related cortical networks were studied with electroencephalography.

The magnitude of the induced oscillatory modulation range in the sensorimotor cortex was independent of both handedness (RH, LH) and hemispheric specialization (DH, NDH). However, the regional beta-band modulation was associated with different alpha-band networks in RH and LH: RH presented a stronger *inter*-hemispheric connectivity, while LH revealed a stronger *intra*-hemispheric interaction. Notably, these distinct network entrainments were independent of hemispheric specialization.

In healthy subjects, sensorimotor beta-band activity can be robustly modulated by motor imagery and proprioceptive feedback in both hemispheres independent of handedness. However, right and left handers show different oscillatory entrainment of cortical alpha-band networks during neurofeedback. This finding may inform neurofeedback interventions in future to align them more precisely with the underlying physiology.

### 1. Introduction

Activation of the cortical motor system in the absence of overt movement using motor imagery and brain-machine interface (BMI) assisted feedback is currently being investigated as a potential therapeutic intervention for stroke patients with persistent motor deficits. This approach is based on the rationale that sensorimotor oscillations show typical patterns of event-related desynchronization (ERD) and synchronization (ERS) during both motor execution and imagery [Pfurtscheller and Lopes da Silva, 1999]. Notably, these fluctuations were shown to be modified by aging and neurological disorders. During healthy aging, baseline power levels of spontaneous beta oscillations were elevated with a concurrent increase of the magnitude of movement-related ERD,

thereby suggesting that a specific beta power threshold needed to be reached for movement execution [Rossiter et al., 2014b; Heinrichs-Graham et al., 2016]. After stroke, the movement-related beta ERD/ERS modulation range was compromised proportionally to the motor impairment level, thereby providing a potential physiological target for therapeutic interventions [Rossiter et al., 2014a; Shiner et al., 2015].

Functionally relevant modulations of cortico-muscular coherence in the oscillatory beta-band were, furthermore, detected in patients with long-term, severe motor deficits after BMI assisted rehabilitation training [Belardinelli et al., 2017]. Moreover, a frequency-specific correlation between sensorimotor beta-band dynamics modulated by BMI neurofeedback and subsequent improvements in an actual motor task was recently demonstrated [Naros et al., 2016; Naros and Gharabaghi, 2015].

*Abbreviations:* DH, dominant hemisphere; EEG, electroencephalographic; ERD, event-related desynchronization; ERSP, event-related spectral perturbation; iCOH, imaginary coherence; LH, left-hander; ME, motor execution; MI, motor imagery; NDH, non-dominant hemisphere; PMC, premotor cortex; PSI, phase slope index; RH, right-hander RH.

\* Corresponding author. Division of Functional and Restorative Neurosurgery, Eberhard Karls University, Otfried-Mueller-Str.45, 72076, Tuebingen, Germany.

E-mail address: [alireza.gharabaghi@uni-tuebingen.de](mailto:alireza.gharabaghi@uni-tuebingen.de) (A. Gharabaghi).

<https://doi.org/10.1016/j.neuroimage.2019.03.067>

Received 1 July 2018; Received in revised form 2 March 2019; Accepted 27 March 2019

Available online 2 April 2019

1053-8119/© 2019 Elsevier Inc. All rights reserved.

Such a correlation was, however, not observed between, e.g., alpha activity (another biomarker often used for BMI interventions) and motor performance. Promoting the ability to voluntarily control beta-oscillations on the basis of proprioceptive feedback might, therefore, improve motor control by facilitating the communication between the motor cortex and muscles in the same frequency band [Kraus et al., 2016a; Royter and Gharabaghi, 2016; Romei et al., 2016; Gharabaghi, 2016; Darvishi et al., 2017; Khademi et al., 2018].

Beta power neurofeedback tasks might, however, be frustrating even for healthy subjects [Fels et al., 2015] and proved to be particularly challenging to stroke patients due to their compromised modulation range [Gomez-Rodriguez et al., 2011; Brauchle et al., 2015]. Frustration and challenge in these neurofeedback studies may, however, also be related to intrinsic factors such as hemispheric dominance. The participants in previous studies were usually right-handers (RH), but trained either their dominant (left) or non-dominant (right) hemisphere (DH, NDH). Specifically, healthy participants [Fels et al., 2015] and stroke patients [Gomez-Rodriguez et al., 2011; Brauchle et al., 2015] in previous studies trained robotic control of their left upper extremity with the non-dominant right hemisphere. The reported limitations may therefore, at least in part, be related to hemispheric dominance. Along these lines, right-handed healthy subjects in another study performed motor imagery of either hand and showed greater beta desynchronization for right hand motor imagery in the left motor cortex than vice versa [Buriánová et al., 2013]. This limited magnitude of imagery-related neural activation in the right hemisphere may be explained by either handedness, i.e., dominance of the left hemisphere in right-handers, or by general hemispheric differences.

To test these hypotheses, we investigated the beta modulation range of each hemisphere with a neurofeedback intervention in both right- and left-handers. Furthermore, we studied oscillatory entrainment of cortical network connectivity to elucidate task-related intra- and interhemispheric interactions.

## 2. Methods

### 2.1. Subject recruitment

We recruited 25 healthy subjects (mean age =  $25.9 \pm 3.7$  years, 7 female). Handedness was assessed using the Edinburgh Handedness Inventory [Oldfield, 1971]. Subjects were assigned into two groups of either consistent right-handers (score  $\geq 70$  in the Edinburgh Handedness Inventory) or consistent left-handers (score  $\leq -70$  in the Edinburgh Handedness Inventory). This resulted in the participation of twelve right-handed (Edinburgh mean score of  $84.2 \pm 10.8$ , maximal score of +100) and nine left-handed (Edinburgh mean score of  $-86.1 \pm 15.3$ , maximal score of -100) subjects in this study. Four subjects had to be excluded from the study since they did not fulfill the inclusion criteria with regard to handedness. The motor imagery ability of subjects participating in this study was assessed using the KVIQ [Malouin et al., 2007] and revealed no significant differences between right- and left-handers. Subjects gave their written informed consent before participation and received financial compensation. The study protocol was approved by the ethics committee of the Medical Faculty of the University of Tuebingen.

### 2.2. Data acquisition

All subjects were comfortably seated upright in a chair. Scalp electroencephalographic (EEG) potentials were recorded (Brain Amp, Brain Products GmbH, Germany) from 32 positions in accordance with the international 10–20 system (Fig. 1 A): Fp1, Fp2, F3, Fz, F4, FT7, FC5, FC3, FC1, FC2, FC4, FC6, FT8, C5, C3, C1, Cz, C2, C4, C6, TP7, CP5, CP3, CP1, CPz, CP2, CP4, CP6, TP8, P3, Pz, POz, with active Ag/AgCl electrodes (acti CAP, Brainproducts GmbH, Germany). FCz was used as a common reference and grounded to AFz. All impedances were kept

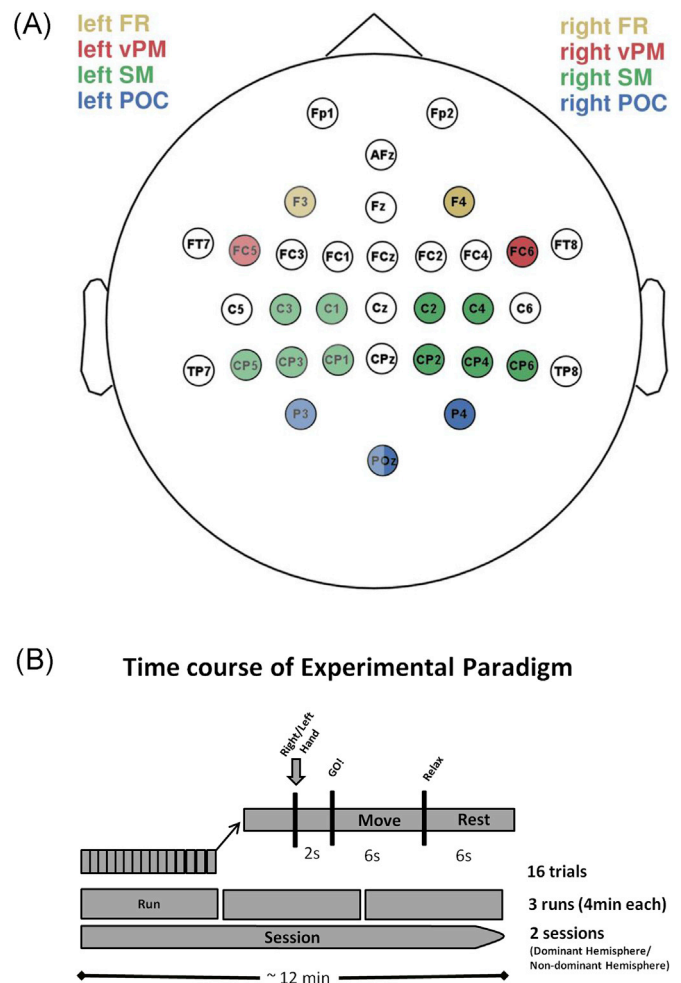


**Fig. 1.** A) Map of EEG channels' location with FR, vPM, SM, and POC referring to electrode locations projecting to frontal, ventral premotor, sensorimotor and parieto-occipital areas, respectively. B) **Experimental paradigm:** Time course of the experimental paradigm, with two randomized sessions of brain self-regulation, one with the volitional control of the dominant hemisphere and the other with the volitional control of the non-dominant hemisphere.

below 20 k $\Omega$  at the onset of each session. EEG data was digitized at 1 kHz, high-pass filtered with a time constant of 10sec, transmitted to the BCI2000 software for online processing and stored for off-line analysis. The code from the toolbox is available online [<http://www.schalklab.org/research/bci2000>; Schalk et al., 2004].

### 2.3. Experimental paradigm

Subjects performed one session with imagery of the right hand and one session with imagery of the left hand, thereby modulating regional brain activity in the dominant and non-dominant hemisphere, respectively.

During the task, subjects were attached to a robotic hand orthosis (Amadeo<sup>®</sup> system, Tyromotion GmbH, Austria). This orthosis was used to open the hand, i.e., providing closed-loop visual and haptic/proprioceptive feedback contingent to volitional modulation of regional sensorimotor beta ( $\beta$ )-oscillations induced by MI [Vukelić et al., 2014; Gharabaghi et al., 2014]. Contingent feedback to successful volitional modulation meant that as soon as the predefined ERD level was achieved, the participants were rewarded by the robotic opening of the hand which they saw and felt. However, if the targeted brain state could not be sustained, the robotic movement ceased again but could be resumed within the same trial if the predefined brain state was attained again

[Naros et al., 2016]. Subjects were instructed to perform kinesthetic MI [Neuper et al., 2005] throughout the MI period. This resulted in event-related desynchronization of  $\beta$ -oscillations ( $\beta$ -ERD) over contralateral sensorimotor regions [Pfurtscheller and Lopes da Silva, 1999]. The subjects were also instructed to observe the robotic hand as it opened. This incorporation of feedback from multiple sensory modalities has been shown to significantly enhance volitional brain control [Suminski et al., 2010; Vukelić and Gharabaghi, 2015a; Brauchle et al., 2015].

The sessions were randomized across the subjects. Each session consisted of three runs of 4 min with each run separated into sixteen trials. Each trial consisted of a cued task design with different task epochs, where an auditory cue was used to indicate the beginning of each epoch. Every trial was initiated by a preparatory epoch (2s, indicated by a Right/Left hand auditory cue), followed by a MI epoch of hand opening (6s, indicated by a GO auditory cue), and completed by a rest period (6s, indicated by a Relax auditory cue). The participants performed motor imagery throughout the 6 s MI period. Fig. 1 B provides an overview of the experimental paradigm. For the online classification of successful  $\beta$ -modulation, an adaptive linear classifier was used as described previously [Vukelić et al., 2014; Gharabaghi et al., 2014]. In short, during each trial, the spectral oscillatory power of the preceding 500 ms was estimated every 40 ms using an autoregressive model based on the Burg Algorithm with a model order of 32 [McFarland and Wolpaw, 2008]. During each session, we used 9 features for our linear classification consisting of 2-Hz frequency bins (16–22 Hz) and three channels overlying sensorimotor areas contralateral to the movement imagery of right- (FC3, C3, and CP3) or left-hand (FC4, C4, and CP4). A decrease in spectral  $\beta$ -power ( $\beta$ -ERD) during the MI epoch was estimated relative to the average power of the rest and preparation phases of the last 15s.

When a predefined (see below) level of  $\beta$ -ERD was classified in five consecutive 40 ms epochs (i.e., 200 ms of consistent  $\beta$ -ERD), the robotic orthosis extended the fingers of the hand. When the predefined level of  $\beta$ -ERD was not achieved, the orthosis stopped, thus resulting in contingent closed-loop haptic feedback to MI. At the end of the trial, the orthosis returned to the starting position. To account for different abilities of  $\beta$ -band modulation, we identified the strongest individual  $\beta$ -ERD of each participant by performing one training run for calibration prior to the experiment. From this calibration run, we defined three threshold values representing different difficulty levels, i.e., the 50% (low difficulty), 30% (moderate difficulty), or 10% (high difficulty) of the strongest, subject-specific  $\beta$ -ERD, respectively. In the following experimental runs, feedback was provided only when the subjects reached either 50% (first run), 30% (second run), or 10% (third run) of their strongest  $\beta$ -ERD. Thereby, the difficulty level increased subsequently throughout the session, ensuring that the participants remained in the deliberative phase of skill acquisition with high demands for volitional brain modulation [Bauer and Gharabaghi, 2015a, b; 2017; Bauer et al., 2016a, b]. To minimize the influence of muscular activity, subjects were instructed not to perform any movements. This was ensured by monitoring online bilateral forearm muscle activity of the Flexor Carpi Radialis (FCR) and Extensor Carpi Radialis (ECR) muscles.

#### 2.4. Data pre-processing

All runs were grouped together, resulting in an EEG data stream of 12 min per subject. Artifacted EEG channels, as determined by visual inspection, were removed. Altogether, we excluded eight EEG channels (Fp1, Fp2, FT7, FT8, C5, C6, TP7, and TP8) from offline-analysis to maintain the same number of channels in each subject. We used two temporal windows for the analysis of the cortico-cortical connectivity: rest epoch (6 s) and MI epoch (6 s). Epochs were rejected if they contained a maximum deviation above  $60 \mu\text{V}$  in any of the EEG channels [Sanei, 2007] or if muscular activity ( $\pm 0.015 \text{ mV}$ ) contralateral to movement was detected. The EEG signals were detrended, zero-padded and band-pass filtered between 1 and 48 Hz for calculation of

imaginary coherence (iCOH) [Nolte et al., 2004] across frequencies. A frequency filter of 6–16 Hz was chosen for the calculation of effective connectivity in the alpha ( $\alpha$ )-frequency range using the phase slope index. For calculation of event-related spectral perturbation (ERSP), signals were band-pass filtered between 14 and 24 Hz. The filtering procedures were performed with a first order zero-phase lag FIR filter as implemented in the signal processing toolbox of MATLAB<sup>®</sup>.

#### 2.5. Calculation of $\beta$ -modulation range

The frequency band and the EEG electrodes implemented in self-regulation and neurofeedback were also applied to calculate the individual  $\beta$ -modulation range for each subject as a performance measure of the ability for volitional brain modulation as introduced previously [Vukelić et al., 2014]. We consider the  $\beta$ -modulation range to be a more physiological biomarker for feedback in cognitive and motor domains than ERD alone, since both the down- and the up-regulation of  $\beta$ -oscillations are functionally relevant and linked to GABA-A and GABA-B-mediated processes, respectively [Muthukumaraswamy et al., 2013]. This approach accounted for the inter-individual variability of different spectral  $\beta$ -peaks in the time course of the different task epochs. The individual  $\beta$ -modulation range was based on calculating offline the ERSP between 16 and 22 Hz with a frequency resolution of 0.24 Hz as implemented in the EEGLAB toolbox [Delorme and Makeig, 2004]. The code from the toolbox is available online [<https://scn.ucsd.edu/eeeglab/index.php>]. The ERSP was estimated according to

$$ERSP(f, t) = \frac{1}{n} \sum_{k=1}^n |F_k(f, t)|^2$$

where  $n$  is the number of electrodes used and  $F_k(f, t)$  the short-time Fourier transform for electrode  $k$ . We calculated the ERSP trial-wise and visualized across time with  $-8$  to  $-2$  s of rest epoch,  $-2$  to  $0$  s of preparatory epoch, and  $0$ – $6$  s of MI epoch. This ERSP map was averaged over the contralateral feedback electrodes (FC3/C3/CP3 or FC4/C4/CP4) for each frequency bin. Since the online classification consisted of the detection of  $\beta$ -ERD during the MI epoch relative to the average of the rest and preparation epochs, we estimated the individual  $\beta$ -modulation range accordingly. By including the preparatory phase of the task, we could provide feedback to the  $\beta$ -ERS also, thereby enhancing the achievable  $\beta$ -modulation range, i.e., the maximum difference between ERD and ERS. The modulation range was not affected by the baseline selection in the same way as the ERD. Furthermore, this rescaling had the benefit of facilitating the use of a fixed threshold for the feedback throughout the experiment as the power estimate was normalized. Moreover, due to this normalization approach, tonic beta-power changes had less influence on the estimates. By using the very same methodology we could show in our previous work that a brain-machine interface might offer a way to bridge the gap between two distinct abilities and cortical alpha-band networks underlying motor control, i.e., a motor imagery network and a motor execution network [Bauer et al., 2015].

More specifically, we estimated the individual frequency bin of the ERSP with the largest difference between the minimum in the MI epoch (describing the maximum desynchronization potential) and the maximum in the rest and preparatory epoch (describing the maximum synchronization potential). This magnitude thus reflected the ability of maximally modulating sensorimotor brain activity during the task. Finally, we averaged the ERSP across trials on an individual basis and across the subject's individual maximum  $\beta$ -modulation range on a group level, resulting in a  $\beta$ -modulation range for MI related modulations of the dominant and the non-dominant hemisphere, respectively.

#### 2.6. Estimation of cortico-cortical connectivity

The estimation of the iCOH and PSI functions were based on an estimation of the complex coherency function, with neither of the

measures being prone to problems of volume conduction [Nolte et al., 2004; Nolte et al., 2008]. More specifically, iCOH makes it possible to inspect the whole spectrum and represents a robust functional connectivity measure ignoring relations at zero phase lag and therefore indicating only the relative coupling of phases, i.e., the time-lag between two brain processes [Nolte et al., 2004]. iCOH was applied to derive a suitable frequency band for the subsequent analysis with the final outcome measure of our study, i.e., the phase slope index (PSI) [Nolte et al., 2008]. Statistics were therefore calculated for the PSI only. PSI represents a more sophisticated connectivity approach that provides further information about the direction of causal relations among brain processes, i.e., effective connectivity, by giving an average of the phase slope spectrum between two time series [Nolte et al., 2008].

For the estimation of the complex coherency function, each valid epoch was subdivided into segments of 1 s length with 50% overlap, corresponding to a frequency resolution of  $\delta f = 1$  Hz [Nolte et al., 2004; Nolte et al., 2008]. Overlapping the segments increases the dependency between segments. However, this is not an issue for PSI. Overlapping segments are asymptotically unbiased and are able to reduce noise (at the cost of frequency resolution). A smooth spectrum is essential since the linear phase-slope is then less affected by noisy estimates. Furthermore, overlapping segments reduce the loss of data when one segment is rejected due to artifacts.

Each segment was multiplied by a Hanning window. A Fourier transformation of the data resulted in an estimation of the cross-spectra between two time-series [Nolte et al., 2004; Nolte et al., 2008]. The complex coherency function was defined as the normalized cross-spectrum for channels  $i$  and  $j$ , respectively:

$$C_{ij}(f) = \frac{S_{ij}(f)}{\sqrt{S_{ii}(f)S_{jj}(f)}}$$

where  $S_{ij}(\cdot)$  was the cross-spectrum between channels  $i$  and  $j$ , and  $S_{ii}(\cdot)$ ,  $S_{jj}(\cdot)$  represented the auto-spectra for channels  $i$  and  $j$ , respectively. Robust estimates of the probability of stable phase lags across frequencies (likelihood of stable phase lags, see Figs. 3 and 4) were obtained by averaging the absolute value of the iCOH function across frequencies of the rest and MI epoch, respectively. This established the probability that certain frequencies show stable phase lags (presence or absence of neuronal communication) among electrode sites, therefore indicating persistent and consequently activated connections during both rest and MI epochs, respectively. Here, we used a corrected version of the iCOH function [Ewald et al., 2012]. In addition, we separated this phase lag stability from the noise floor as described by a  $1/f$  noise model [Blankertz et al., 2010]. PSI is defined as the weighted sum of the slope of the phase spectrum of the normalized cross-spectra [Nolte et al., 2008]. We chose the frequency range between 8 and 14 Hz to estimate the effective connectivity in the  $\alpha$ -range on the basis of a pronounced peak above noise floor in the probability of observing stable phase lags in this range. PSI was calculated as originally proposed by [Nolte et al., 2008]:

$$PSI_{ij}(f) = \Im \left( \sum_{f \in F} C_{ij}^*(f) C_{ij}(f + \delta f) \right),$$

where  $C_{ij}$  was the complex coherency between channels  $i$  and  $j$ , and  $\delta f$  was the frequency resolution.  $\Im(\cdot)$  denoted the imaginary part of the coherency while  $F$  was the frequency band over which the slope was summed [Nolte et al., 2008]. This resulted in PSI estimations for all unrejected epochs of the rest and MI phase, respectively. For the estimation of the complex ordinary coherency, a Welch method was used as described above. All data analysis was performed offline with custom written or adapted scripts in MATLAB<sup>®</sup>. The code for calculating PSI is available online [http://doc.ml.tu-berlin.de/causality/, Nolte et al., 2008]. From this code we adopted the calculation of the ciCOH as described in detail above.

## 2.7. Statistical evaluation of cortico-cortical effective connectivity

The sign of PSI indicates whether the channel is a transmitter (positive sign) or a receiver (negative sign), and the sign, but not the magnitude of PSI, is independent from the power fluctuation of the signals. Averaging the sign of PSI across unrejected epochs results in a robust estimation of the likelihood of a connection being either a transmitter or a receiver, which is indicative of a persistent and thus stable direction of transmission throughout the rest and MI epochs, respectively. Bearing this in mind, the probability that a connection between two channels  $i$  and  $j$  is transmitting or receiving, i.e., the likelihood of phase slope index (LPSI) was calculated as follows:

$$LPSI_{ij}(f) = \frac{\sum_e \text{sgn} \left( \Im \left( \sum_{f \in F} C_{ij}^*(f, e) C_{ij}(f, e + \delta f) \right) \right)}{E}$$

where  $e$  and  $E$  represent the number of epochs over which the sign (sgn) was averaged. This resulted in LPSI scores for the rest and MI epochs, respectively. To account for the low number of samples and the subsequent possibility of non-normality, we used an empirical distribution technique, i.e., a surrogate data approach [Kamiński et al., 2001; Babiloni et al., 2005; Haufe et al., 2013]. For the surrogates, we chose the original data, in which the temporal order had been randomly permuted separately for each channel time series and for each unrejected epoch of the subjects. This procedure destroys all the temporal structure within a time series as well as the interdependency between the time series and affords the PSI estimates the opportunity to establish a null distribution. PSI estimates were then calculated from this randomly and independently shuffled time series. The shuffling procedure was performed 1000 times for each subject and epoch (rest and MI separately) and, finally, averages of LPSI scores across the surrogates were taken into consideration. Hence, we were able to perform two sided t-tests on the differences of connectivity scores obtained on original and permuted data [Haufe et al., 2013] assuming an alpha error of  $p < 0.05$  as significant, corrected for multiple comparisons by limiting the false discovery rate (FDR) to 5% [Benjamini and Hochberg, 1995].

## 3. Results

### 3.1. Beta modulation range in both hemispheres is independent of handedness

Fig. 2A and B show the ERSP during MI related sensorimotor  $\beta$ -modulations of the dominant hemisphere (DH) and the non-dominant hemisphere (NDH) in RH (upper plots) and LH (lower plots), respectively. The plots illustrate that both groups displayed a strong decrease of  $\beta$ -power over contralateral sensorimotor cortices during the MI epoch in comparison to the rest epoch. Both groups showed their maximal synchronization during the preparatory epoch. Fig. 2C shows the ability for MI-related  $\beta$ -modulations of regional sensorimotor areas for both DH and NDH in RH and LH, respectively. We used a two by two ANOVA to ascertain whether the factors Handedness (RH, LH) or Hemispheric Dominance (DH, NDH) had an influence on the distribution of  $\beta$ -modulation range. The RH/LH by DH/NDH ANOVA revealed no significant effects on the differences of the distribution of  $\beta$ -modulation range (see Table 1).

### 3.2. Cortical networks during motor imagery of dominant hand

We observed an increase in the likelihood of stable phase lags over the noise floor in the  $\alpha$ -range (between 8 and 14 Hz) in both RH and LH during the MI and rest epoch (left panel in Fig. 3 A and 3 B). This likelihood decreased with increasing frequency while showing no relevant elevation over the noise floor when monitoring higher frequencies such as  $\beta$ - and  $\gamma$ -activity. The directionality across cortico-cortical sites of these stable phase lags in the  $\alpha$ -range was estimated using the PSI function and

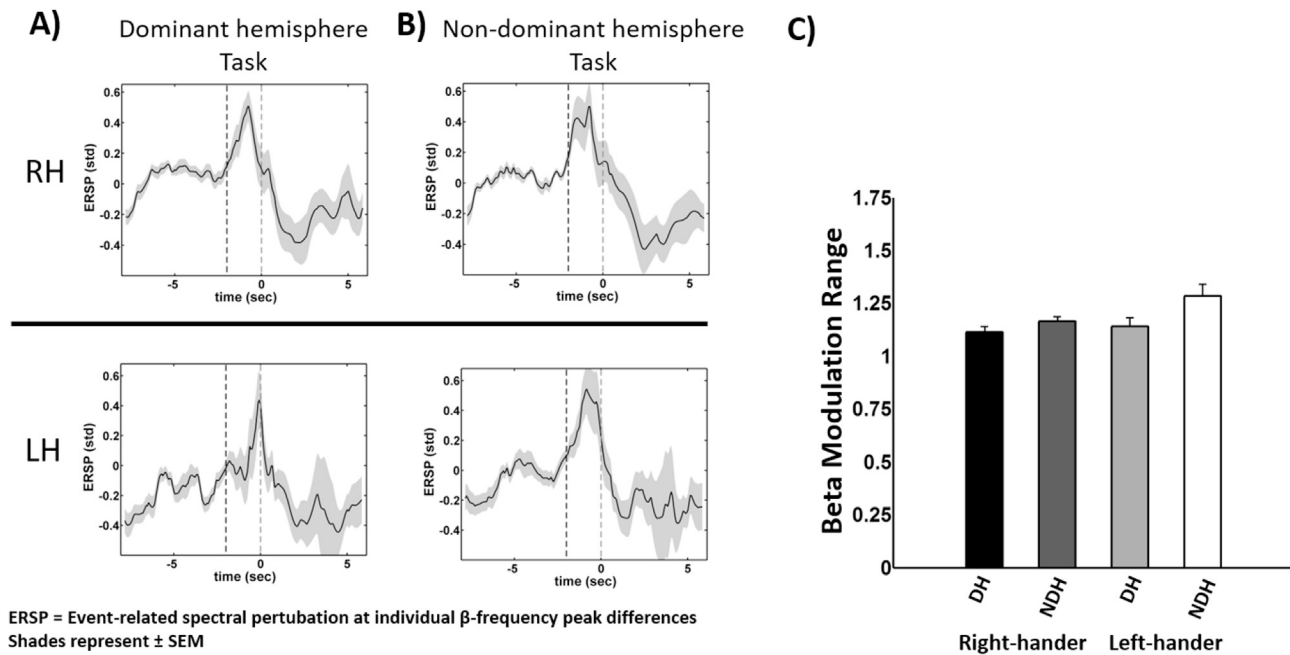


**Fig. 2. Event-related spectral perturbation (ERSP) and the respective  $\beta$ -modulation range.** A) and B) show the results of motor imagery-related  $\beta$ -modulations of the dominant hemisphere (DH) and of the non-dominant hemisphere (NDH), respectively. The upper two plots represent the results for the right-handers (RH) and the lower two plots depict the results for the left-handers (LH). The plots show the time course of the event-related spectral perturbation (ERSP) of the  $\beta$ -oscillations. The abscissa represents the time axis, with the rest epoch from  $-8$  to  $-2$  s (dashed black line), the preparation epoch from  $-2$  to  $0$  s (dashed gray line), and the motor imagery epoch from  $0$  to  $6$  s. The black line (contralateral sensorimotor electrodes) shows the group level results as an average, both across trials on an individual level and across the subject's individual maximum  $\beta$ -modulation range (visualized on a standard deviation (std) scale, and normalized with respect to the rest baseline). Shades represent  $\pm$  SEM. C) The figure shows the mean of the  $\beta$ -modulation range for the two groups (RH and LH) and for both motor imagery-related  $\beta$ -modulations of DH and NDH. Error bars represent  $\pm$  SEM.

**Table 1**

Two by two ANOVA with the factors Handedness (RH and LH) and Hemispheric Dominance (DH and NDH) and with  $\beta$ -modulation range as dependent variable.

Effect	DF(n,d)	F	Prob > F
Handedness	(1,38)	0.86	0.36
Hemispheric Dominance	(1,38)	1.23	0.27
Handedness* Hemispheric Dominance	(1,38)	0.55	0.46

RH and LH have the same ability for volitional modulation of regional sensorimotor  $\beta$ -oscillations for both the DH and the NDH (see Fig. 2).

is illustrated on the right panel in Fig. 3 A and 3 B, separately for the MI (left figures) and rest epoch (right figures) as a global average across RH and LH, respectively.

During the MI epoch, RH showed prominent information flow between CP5/CP3/CP1 and P3/POz electrodes, referred to as SM (sensorimotor) and POc (parieto-occipital), respectively. It should, however, be borne in mind that the acronyms (e.g., SM) that are applied for the electrode groups in this study are used in a descriptive way only. Furthermore, RH exhibited conspicuous interhemispheric information flow between C1/C3/CP1/CP5 and FC6 electrodes, referred to as SM and vPM (ventral premotor), respectively, as well as between C2/C4 and FC6 electrodes. During the rest epoch, RH indicated information flow between CP3/CP5/CPz and P3/POz electrodes.

By contrast, LH exhibited strong bilateral intra-hemispheric coupling during the MI epoch between C2/C4/CP1/CP2/CP4/CP6/CPz and P3/P4/POz electrodes. This effect was more pronounced in the contralateral hemisphere. The bilateral intrahemispheric coupling was similarly activated during the rest epoch in LH.

### 3.3. Cortical networks during motor imagery of non-dominant hand

Sensorimotor  $\beta$ -modulations of the NDH showed a pronounced

increase in the likelihood of stable phase lags over the noise floor in the  $\alpha$ -range (between 8 and 14 Hz) for both RH and LH during the MI and the rest epoch, (left panel in Fig. 4A and B). Furthermore, when monitoring higher frequencies from  $\beta$ -to  $\gamma$ -range, this likelihood showed no relevant elevation over the noise floor. The right panel depicts the topographical causal interactions across cortico-cortical sites in the  $\alpha$ -range, separately for the MI epoch (left figures) and the rest epoch (right figures) as a global average across RH and LH, respectively.

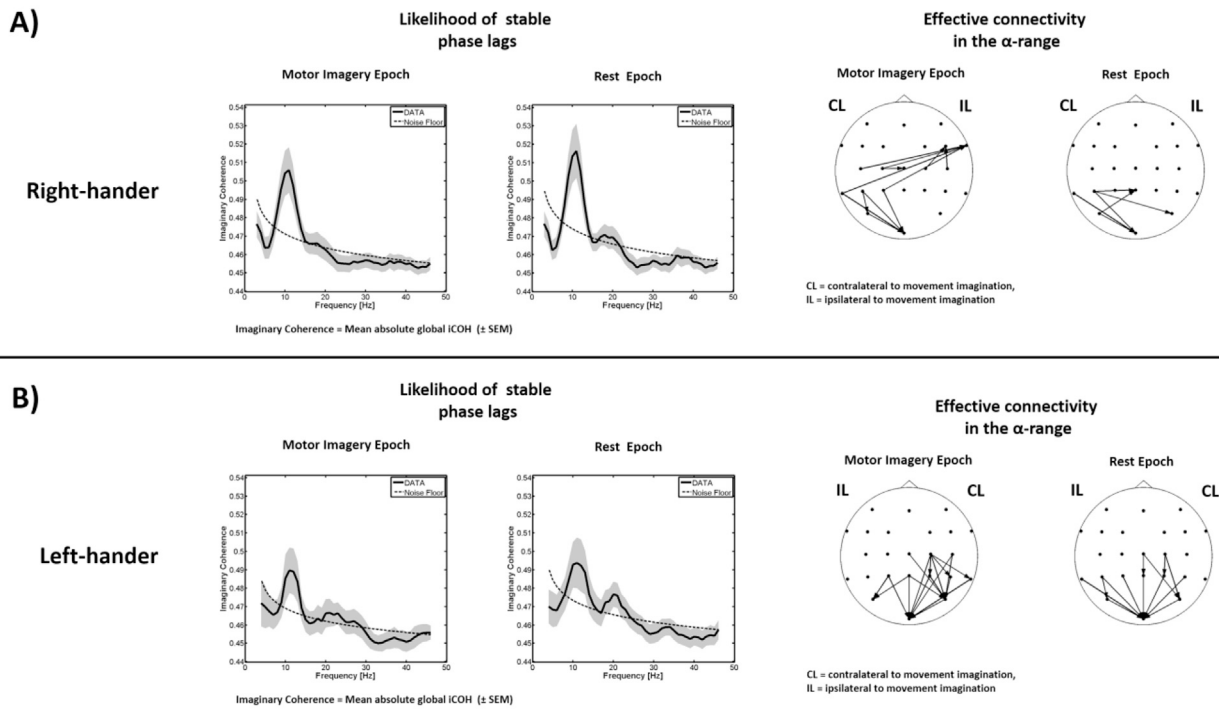
During the MI epoch, a pronounced information flow was observed in RH between CP4/CP5/CP6 and P3/P4/POz electrodes. Furthermore, F3 and FC5 electrodes, referred to as FR (ipsilateral frontal) and vPM, respectively, received information from C2/C4/CPz/CP2/CP4/CP6 electrodes. During the rest epoch, RH showed contralateral information flow between CP4/CP6 and P4/POz electrodes.

On the other side, LH engaged in a strong bilateral intra-hemispheric information flow between CP4/CP5/CP6 and P3/P4/POz electrodes as well as between midline Fz and CP4/CP5/CP6 electrodes during the MI epoch. During the rest epoch, LH exhibited contralateral information flow between CP4/CP5/CP6 and P3/P4/POz electrodes.

### 3.4. Different neuronal strategies

We analyzed the results with a two by two ANOVA to test the factors (RH/LH and DH/NDH) with regard to their impact on the distribution of the likelihood (LPSI scores) of information flow during the MI epoch. Hence, the *inter*-hemispheric and the *intra*-hemispheric information flow were grouped according to regions of interest. In particular, we defined *inter*-hemispheric information flow (communication between the two hemispheres) as crossing midline central electrodes, while *intra*-hemispheric information flow (communication within each hemisphere) was defined as not crossing midline central electrodes, as specified in detail below.

We therefore averaged the LPSI scores of transmission from C2/C4/

Cortical networks during motor imagery of *dominant* hand

**Fig. 3. Cortical networks during motor imagery of the dominant.** A) and B) depict the results of right-handers and left-handers, respectively. The figures on the left represent the likelihood of stable phase lags across frequencies (abscissa). The solid black lines represent the mean global (average across all connections) iCOH as an average over all subjects during the motor imagery (left side) and rest epoch (right side), respectively. The dashed black lines represent the estimated noise floor as explained by a  $1/f$  noise model [45]. Shades represent  $\pm$  SEM. The maximum elevation over the noise floor of phase lag stability is located in the  $\alpha$ -band (between 8 and 14 Hz). The two figures on the right illustrate the stable topographical causal interactions (arrows indicate significant cortical information flow,  $p < 0.05$  FDR corrected for multiple comparison) of the  $\alpha$ -band networks as a global average across all subjects during the motor imagery (left side) and rest epoch (right side), respectively.

CP2/CP4/CP6 (right SM) to F3/FC5 (left FR/vPM) electrodes during the MI epoch for each subject. The probability of interhemispheric SM-FR information (Right SM-Left FR) flow for both RH and LH and for both DH and NDH are summarized in Fig. 5A. The RH/LH by DH/NDH ANOVA is shown in Table 2. RH showed a higher probability of interhemispheric SM-FR information flow than LH (significant main effect for Handedness  $F_{(1,38)} = 5.13$ ,  $p = 0.02$ ). Furthermore, RH showed a higher probability of interhemispheric SM-FR information flow for NDH than for DH (significant main effect Hemispheric Dominance  $F_{(1,38)} = 5.8$ ,  $p = 0.02$ , post hoc analysis, two sided  $t$ -test,  $p$ -value = 0.01).

We next averaged each subject's LPSI scores of transmission from C1/C3/CP1/CP3/CP5 (left SM) to FC6 (right vPM) electrodes during the MI epoch. The likelihood of interhemispheric SM-vPM information flow (Left SM-Right vPM) for RH and LH and for DH and NDH is shown in Fig. 5B. The RH/LH by DH/NDH ANOVA is shown in Table 3. RH showed a higher likelihood of interhemispheric SM-vPM information flow than LH (significant main effect for Handedness  $F_{(1,38)} = 6.67$ ,  $p = 0.01$ ).

We also averaged the LPSI scores of transmission from C1/C3/CP1/CP3/CP5 and C2/C4/CP2/CP4/CP6 (SM) to P3/POz and P4/POz (POc) electrodes, respectively, during the MI epoch for each hemisphere and subject. This value was taken to be an indicator of intra-hemispheric SM-POc communication. The results of the likelihood of left and right intra-hemispheric SM-POc communication (Left SM-POc and Right SM-POc) for both RH and LH and for both DH and NDH are illustrated in Fig. 5C and D, respectively. The RH/LH by DH/NDH ANOVA for the likelihood of left intra-hemispheric SM-POc information flow as a dependent variable is shown in Table 4. LH showed a

higher left hemispheric SM-POc likelihood than RH (significant main effect for Handedness  $F_{(1,38)} = 8.86$ ,  $p = 0.005$ ). The RH/LH by DH/NDH ANOVA for the likelihood of right intra-hemispheric SM-POc information flow as a dependent variable is shown in Table 5. Again, LH showed the higher likelihood of right intra-hemispheric SM-POc communication (significant main effect for Handedness  $F_{(1,38)} = 11.1$ ,  $p = 0.002$ ).

### 3.5. Ability for volitional $\beta$ -modulation and the neuronal network correlates

The values of the LPSI scores of inter-hemispheric SM-FR and intra-hemispheric SM-POc are plotted against the  $\beta$ -modulation range for RH and LH, respectively in Fig. 6. The two plots in Fig. 6 A illustrate the relationships of MI related sensorimotor  $\beta$ -modulations of DH for RH (left side) and LH (right side), respectively:

In RH, higher likelihoods of *inter-hemispheric* SM-vPM information flow (Left SM-Right vPM) correlated positively with their self-regulation ability (MI related modulations of  $\beta$ -band oscillations of the dominant hemisphere) for the DH (Pearson's correlation coefficient  $r_{ps} = 0.65$ ,  $p$ -value = 0.02). This accounted for as much as 43% of the variance in this ability in RH (linear regression analysis,  $R^2 = 0.43$ ).

In LH, higher likelihoods of *right intra-hemispheric* SM-POc information flow (Right SM-POc) correlated positively with their self-regulation ability (MI related modulations of  $\beta$ -band oscillations of the dominant hemisphere) for the DH (Pearson's correlation coefficient  $r_{ps} = 0.70$ ,  $p$ -value = 0.03). This accounted for 42% of the variance in this ability in LH (linear regression analysis,  $R^2 = 0.42$ ).

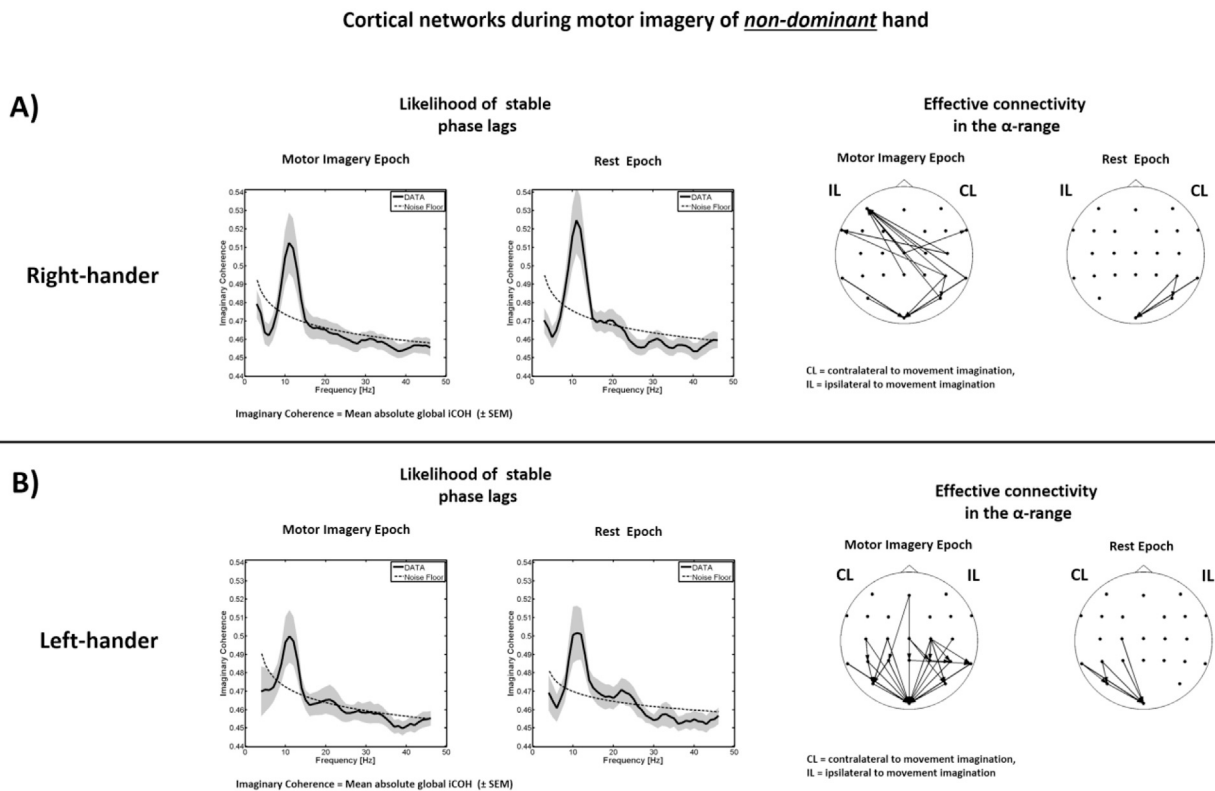


**Fig. 4. Cortical networks during motor imagery of the dominant and non-dominant hemisphere:** **A)** and **B)** depict the results of right-handers and left-handers, respectively. The figures on the left represent the likelihood of stable phase lags across frequencies (abscissa). The solid black lines represent the mean global (average across all connections) iCOH as an average over all subjects during the motor imagery (left side) and rest epoch (right side), respectively. The dashed black lines represent the estimated noise floor as explained by a  $1/f$  noise model [45]. Shades represent  $\pm$  SEM. The maximum elevation over the noise floor of phase lag stability is located in the  $\alpha$ -band (between 8 and 14 Hz). The two figures on the right illustrate the stable topographical causal interactions (arrows indicate significant cortical information flow,  $p < 0.05$  FDR corrected for multiple comparison) of the  $\alpha$ -band networks as a global average across all subjects during the motor imagery (left side) and rest epoch (right side), respectively.

The two plots in Fig. 6B illustrate the relationships between MI-related sensorimotor  $\beta$ -modulations of NDH for RH (left side) and LH (right side), respectively:

In RH, higher likelihoods of *inter-hemispheric* SM-FR information flow (Right SM-Left FR) correlated positively with their self-regulation ability (MI related modulations of  $\beta$ -band oscillations of the non-dominant hemisphere) for the NDH (Pearson's correlation coefficient  $r_{ps} = 0.61$ ,  $p$ -value = 0.03). This accounted for as much as 36% of the variance in this ability in RH (linear regression analysis,  $R^2 = 0.36$ ).

In LH, higher likelihoods of midline Fz to CP1/CPz information flow correlated negatively with their self-regulation ability (MI related modulations of  $\beta$ -band oscillations of the non-dominant hemisphere) for the NDH (Pearson's correlation coefficient  $r_{ps} = -0.75$ ,  $p$ -value = 0.02). This accounted for 50% of the variance in this ability in LH (linear regression analysis,  $R^2 = 0.50$ ).

#### 4. Discussion

This study revealed that both RH and LH could volitionally modulate regional sensorimotor  $\beta$ -oscillations without any significant difference in the distribution of the  $\beta$ -modulation range. This performance was independent of DH and NDH, respectively (Fig. 2). However, RH and LH showed different patterns of network activity between distributed cortical regions during this task. These coherent communications were specific for the oscillatory  $\alpha$ -range (Figs. 3 and 4), in line with the known role of this frequency band for sensorimotor behavior [Jensen and Mazaheri, 2010; Capotosto et al., 2009; Haegens et al., 2011; Klimesch, 2012; Weisz et al., 2014], integration and information coupling of distant

cortical regions [Palva and Palva, 2011; Pineda, 2005; Bollimunta et al., 2008; Mo et al., 2011; Palva et al., 2011], and task-specific neurocognitive strategies [Smith et al., 1999, 2001]. Moreover, the results supported our previous findings of cross-frequency interactions within the sensorimotor system [Bauer et al., 2015; Vukelić et al., 2014; Vukelić and Gharabaghi, 2015a, b]. The various cortical regions which were active during self-regulation of regional  $\beta$ -activity in RH and LH corresponded to the different areas involved during both imagined and executed movements [Miller et al., 2010; Wander et al., 2013; Averbeck et al., 2009; Gao et al., 2011; Karabanov et al., 2012; Koch et al., 2007]:

In the rest epoch of the task, which included the passive orthotic hand movement to the starting position and the stable rest state, a dominant information flow occurred between contralateral sensorimotor and parieto-occipital regions. This activation of precentral and postcentral regions tallied well with the cortical activation pattern for passive wrist movements found in earlier studies [Szameitat et al., 2012]. The interconnection of these areas with parietal regions is consistent with the view that the parietal cortex acts as an important node for visuomotor and sensorimotor integration, providing information about the current state of the hand by integrating sensory feedback [Gandolla et al., 2014].

##### 4.1. Regional event-related modulation of $\beta$ -power

As anticipated, we observed  $\beta$ -power synchronization in the preparatory and relaxation epoch, and  $\beta$ -power desynchronization in the MI epoch. The desynchronization of  $\beta$ -power has already been reported during both ME and MI [McFarland et al., 2000], reflecting the conjunction of several factors related to sensorimotor and cognitive

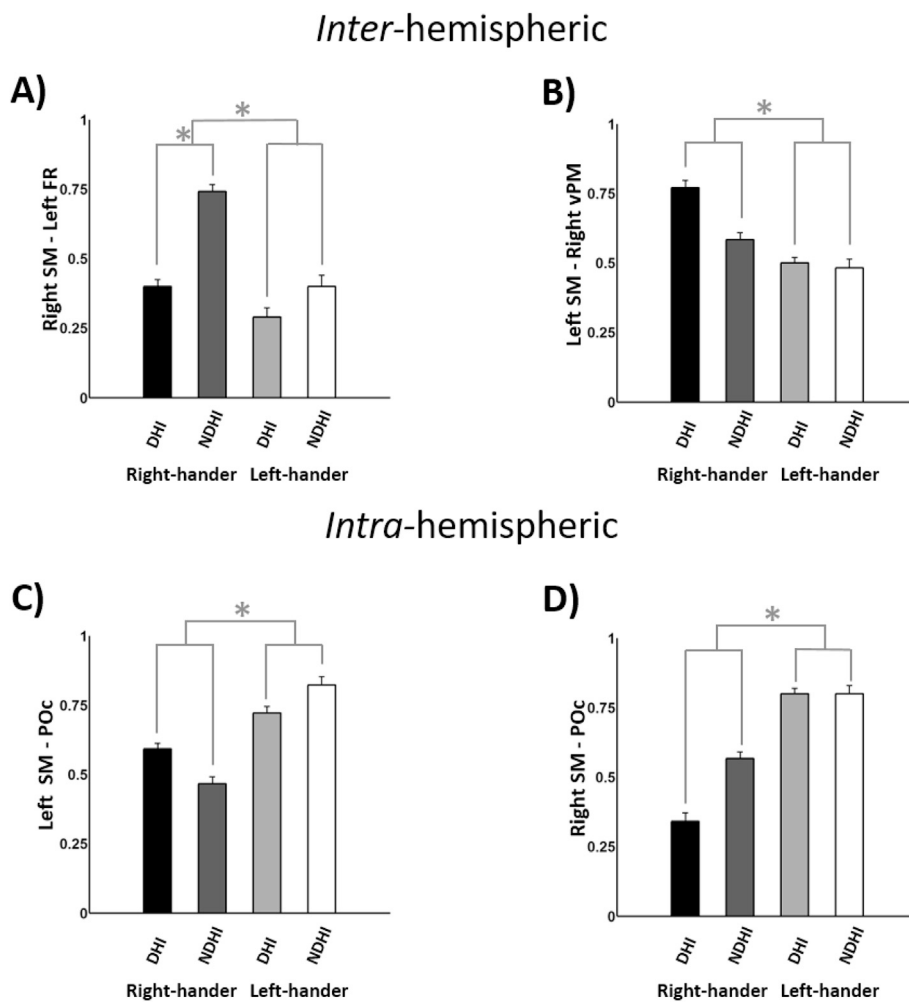


**Fig. 5. Different neuronal strategies; A):** The mean likelihood (LPSI scores) of interhemispheric sensorimotor-frontal (Right SM-Left FR) communication during the motor imagery epoch is shown. \* indicates significant effects (see Table 2). Error bars represent  $\pm$  SEM. **B):** The figure shows the mean likelihood (LPSI scores) of interhemispheric sensorimotor-ventral premotor (Left SM-Right vPM) communication during which the motor imagery epoch. \* indicates significant effects (see Table 3). Error bars represent  $\pm$  SEM. **C):** The figure represents the mean likelihood (LPSI scores) of left intrahemispheric sensorimotor-parieto-occipital (Left SM-POc) communication during which the motor imagery epoch. \* indicates significant effects (see Table 4). Error bars represent  $\pm$  SEM. **D):** The figure depicts the mean likelihood (LPSI scores) of right intrahemispheric sensorimotor-parieto-occipital (Right SM-POc) communication during which the motor imagery epoch. \* indicates significant effects (see Table 5). Error bars indicate  $\pm$  SEM. DHI and NDHI indicate dominant hand imagery and non-dominant hand imagery, respectively.

**Table 2**

Two by two ANOVA with the factors Handedness (RH and LH) and Hemispheric Dominance (DH and NDH) and with likelihood (LPSI scores) of right sensorimotor to left frontal (SM-FR) information flow during the motor imagery epoch as dependent variable.

Effect	DF(n,d)	F	Prob > F
Handedness	(1,38)	5.13	0.02
Hemispheric Dominance	(1,38)	5.8	0.02
Handedness* Hemispheric Dominance	(1,38)	0.12	0.73

RH show a higher likelihood of interhemispheric SM-FR communication than LH. Furthermore, RH show a higher likelihood of interhemispheric SM-FR communication when comparing DH and NDH (see Fig. 5A). Post hoc analysis consisted of a two-sided t-test (p-value = 0.01).

**Table 3**

Two by two ANOVA with the factors Handedness (RH and LH) and Hemispheric Dominance (DH and NDH) and with likelihood (LPSI scores) of left sensorimotor to right ventral premotor (SM-vPM) information flow during the motor imagery epoch as dependent variable.

Effect	DF(n,d)	F	Prob > F
Handedness	(1,38)	6.67	0.01
Hemispheric Dominance	(1,38)	0.26	0.61
Handedness* Hemispheric Dominance	(1,38)	2.24	0.14

RH shows a higher likelihood of interhemispheric SM-vPM communication than LH (see Fig. 5B).

**Table 4**

Two by two ANOVA with the factors Handedness (RH and LH) and Hemispheric Dominance (DH and NDH) and with likelihood (LPSI scores) of left sensorimotor to left parieto-occipital (SM-POc) information flow during the motor imagery epoch as dependent variable.

Effect	DF(n,d)	F	Prob > F
Handedness	(1,38)	8.86	0.005
Hemispheric Dominance	(1,38)	0.02	0.88
Handedness* Hemispheric Dominance	(1,38)	1.9	0.18

LH show a higher likelihood of left hemispheric SM-POc communication than RH (see Fig. 5C).

**Table 5**

Two by two ANOVA with the factors Handedness (RH and LH) and Hemispheric Dominance (DH and NDH) and with the likelihood (LPSI scores) of right sensorimotor to right parieto-occipital (SM-POc) information flow during the motor imagery epoch as dependent-variable.

Effect	DF(n,d)	F	Prob > F
Handedness	(1,38)	11.1	0.002
Hemispheric Dominance	(1,38)	1.71	0.19
Handedness* Hemispheric Dominance	(1,38)	0.94	0.33

LH show a higher likelihood of right hemispheric SM-POc communication than RH (see Fig. 5D).

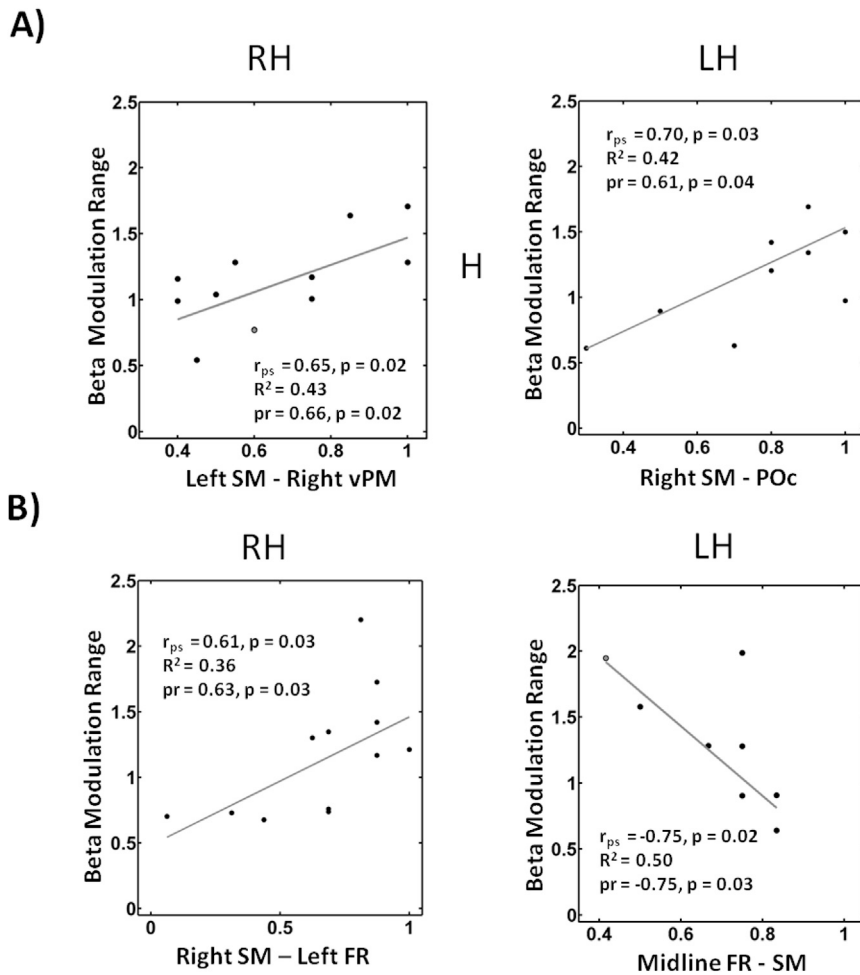


**Fig. 6. Ability of volitional  $\beta$ -modulation and its relation to effective connectivity in the  $\alpha$ -range:**

**A) Motor imagery-related  $\beta$ -modulations of the dominant hemisphere and their neuronal network correlates.** The left scatter plot represents the neuronal network correlates for the right-handed subjects. The  $\beta$ -modulation range is represented on the ordinate where the abscissa indicates the likelihood (LPSI scores) of interhemispheric sensorimotor-ventral premotor (Left SM-Right vPM) communication during the motor imagery epoch. The gray line is the result of a robust regression analysis of the  $\beta$ -modulation range on the likelihood of interhemispheric SM-vPM communication using iteratively reweighted least squares with a bisquare weighting function [Pearson's correlation coefficient  $r_{ps} = 0.65$ ,  $p$ -value = 0.02,  $R^2 = 0.43$ , partial correlation (corrected for hand dominance)  $pr = 0.66$ ,  $p = 0.02$ ]. The gray dot overlying the black indicates two different subjects. The right scatter plot shows the neuronal network correlates for the left-handed subjects. Again, the ordinate illustrates the  $\beta$ -modulation range and the likelihood (LPSI scores) of right hemispheric sensorimotor-parietooccipital (Right SM-POc) communication during the motor imagery epoch is depicted on the abscissa. The gray line is the result of a robust regression analysis of the  $\beta$ -modulation range onto the likelihood of right hemispheric SM-POc communication using iteratively reweighted least squares with a bisquare weighting function [ $r_{ps} = 0.70$ ,  $p$ -value = 0.03,  $R^2 = 0.42$ , partial correlation (corrected for hand dominance)  $pr = 0.61$ ,  $p = 0.04$ ].

**B) Motor imagery-related  $\beta$ -modulations of the non-dominant hemisphere and their neuronal network correlates.** The result of the neuronal network correlates for the right-handers is illustrated on the left scatter plot. Ordinate shows the  $\beta$ -modulation range and abscissa the likelihood (LPSI scores) of interhemispheric sensorimotor-frontal (Right SM-Left FR) communication during the motor imagery epoch. The gray line is the result of a robust regression analysis of the  $\beta$ -modulation range onto the likelihood of interhemispheric SM-FR communication using iteratively reweighted least squares with a bisquare weighting function [ $r_{ps} = 0.61$ ,  $p$ -value = 0.03,  $R^2 = 0.36$ , partial correlation (corrected for hand dominance)  $pr = 0.63$ ,  $p = 0.03$ ]. The right scatter plot illustrates the neuronal network correlates of the left-handers. While the  $\beta$ -modulation range is shown on the ordinate, the likelihood (LPSI scores) of midline fronto-sensorimotor (Midline FR-SM) communication (Fz, to CPz, and CP1) is shown on the abscissa. The gray line is the result of a robust regression analysis of the  $\beta$ -modulation range onto the likelihood of midline FR-SM communication using iteratively reweighted least squares with a bisquare weighting function [ $r_{ps} = -0.75$ ,  $p$ -value = 0.02,  $R^2 = 0.50$ , partial correlation (corrected for hand dominance)  $pr = -0.75$ ,  $p = 0.03$ ]. The gray dot overlying the black indicates two different subjects.

aspects of motor control, and indicating the activation of the sensorimotor system in association with an increase in cortical and peripheral communication [Kilavik et al., 2013; Baker et al., 2003; Jackson et al., 2002]. The synchronization of  $\beta$ -power during the relaxation epoch following MI is related to the same physiological mechanism as the  $\beta$ -rebound after movement execution [Pfurtscheller and Solis-Escalante, 2009; Solis-Escalante et al., 2012]. This is indicative of an active inhibition of the regional sensorimotor areas following termination of a motor program, i.e., MI of hand movements. By contrast, the  $\beta$ -power

increase during the preparatory epoch might reflect regional communication for an efficient preparation or an anticipatory up-regulation of attention in the sensorimotor system before the MI epoch [Kilavik et al., 2013]. Therefore, our results indicate that RH and LH apply similar strategies for the event-timing of regional modulations of  $\beta$ -oscillations for their respective DH and NDH, resulting in the same self-regulation performance regardless of handedness and hemispheric dominance. In future, a combination of this exploration of task-related oscillatory properties with complementary mapping approaches such as refined

transcranial magnetic stimulation techniques [Kraus and Gharabaghi, 2015; Mathew et al., 2016] may elucidate how hemispheric similarities in sensorimotor  $\beta$ -self-regulation relate to hemispheric differences of the cortical motor map [Kraus and Gharabaghi, 2016].

#### 4.2. Large-scale neuronal signatures underlying self-regulation of regional brain activity in right- and left-handers

In the present study on volitional  $\beta$ -band modulation, the maximum elevation of task-related cortical networks above the noise floor, i.e., “likelihood of stable phase lags”, was present in the  $\alpha$ -band (Figs. 3 and 4). This finding is in line with previous imaging studies based on multi-channel electroencephalography. They revealed several cross-frequency interactions as summarized previously [Gharabaghi, 2016]: The sensorimotor  $\beta$ -band self-regulation and BMI feedback entrained an extended cortical  $\alpha$ -network that included frontal and parietal brain areas [Vukelić et al., 2014; Vukelić and Gharabaghi, 2015a] with distributed but spatially selective and frequency-specific effects on cortico-cortical connectivity that lasted beyond the intervention period [Vukelić and Gharabaghi, 2015b]. This cross-frequency interaction in the motor network was critically linked to the proprioceptive feedback provided by the BMI [Vukelić and Gharabaghi, 2015a]. Notably, those subjects who were particularly capable of performing sensorimotor brain self-regulation in the  $\beta$ -band could be predicted by a distributed  $\alpha$ -band resting state network measured before the intervention [Bauer et al., 2015].

Since subjects needed to volitionally control their current neuronal state, this can be considered a cognitively demanding task that engaged distributed network beyond the motor area [Smith et al., 1999, 2001; Halsband and Lange, 2006]. At the same time, this exercise also bears a certain similarity to a motor task, especially when providing subjects with haptic/proprioceptive feedback in a brain-robot interface environment. In this context, the feedback serves several purposes: explicit learning involving sensory processing, online monitoring, acquisition of motor skills and consolidation of motor memory [Dobkin, 2004; Krakauer and Mazzoni, 2011; Lalazar and Vaadia, 2008]. We intentionally increased the task difficulty in our study to maximize volitional modulation of  $\beta$ -band oscillatory activity over sensorimotor regions. Even though RH and LH showed the same ability for regional brain control of  $\beta$ -oscillations, distinct large-scale signatures of connectivity were found in the  $\alpha$ -range during the MI epoch of the task differentiating RH and LH. RH showed a stronger inter-hemispheric connectivity than LH while LH revealed a stronger intra-hemispheric interaction than RH (Figs. 3–5). This might indicate that RH and LH employed different neuronal strategies for regional brain control independent of the self-regulated hemisphere. This is in line with previously reported differences between RH and LH for mental simulations and mental rotation tasks of dominant and non-dominant hand movements [De Nooijer et al., 2013; Gonzalez et al., 2008; Ionta and Blanke, 2009; Ionta et al., 2007]. This is also supported by the correlational analyses (Fig. 6), which were performed in an exploratory way. The respective findings should therefore be interpreted with caution and serve only as an indicator for further studies by pointing to possible links between cortical networks and the sensorimotor modulation range.

In our study, RH integrated the information flow between sensorimotor and parieto-occipital regions in the contralateral hemisphere as well as between sensorimotor, frontal and premotor regions of both hemispheres. The information flow between these regions was not influenced by hemispheric dominance, i.e., the connectivity pattern remained unchanged regardless of whether the dominant or the non-dominant hemisphere was modulated. The interhemispheric communication during the control of the dominant hemisphere might indicate that neurocognitive strategies that rely on recall of motor memory related networks are at work [Halder et al., 2011; Suzuki, 2007]. The two premotor cortices (PMC) are responsible for different aspects of motor learning [Hardwick et al., 2013]. The right PMC is mainly involved in advanced stages of learning and during recall of motor sequences of

familiar motor sequences, while the left PMC is primarily involved in the acquisition of new motor sequences, particularly of unfamiliar movements [Hardwick et al., 2013; Schubotz and von Cramon, 2003]. Furthermore, a dorso-ventral gradient for leg and foot, arm with hand and, finally, face representations in PMC exists that is akin to the topological representation in primary sensorimotor cortices [Graziano et al., 2002a, b]. The human ventral PMC (vPMC) is proportionally much larger than the dorsal PMC (dPMC) [Schubotz and von Cramon, 2003], and the activation of vPMC is consistently involved in paradigms requiring MI and movement observation [Szameitat et al., 2012; Buccino et al., 2001; Jeannerod, 2001].

Hence, when RH volitionally modulated the *dominant hemisphere*, the information flow between left sensorimotor and right vPMC plausibly represented the integration of the imagined movement of the own hand with the current state of sensorimotor features, i.e., interpreting and comparing inflow of haptic/proprioceptive information with the memory of past familiar movements [Christensen et al., 2007; Vahdat et al., 2011]. On the other hand, when RH volitionally modulated the *non-dominant hemisphere*, the information flow between right sensorimotor to left vPMC and frontal cortices might indicate short-term storage of sensorimotor information [Eliassen et al., 2000; Shadmehr and Holcomb, 1997].

By contrast, LH employed synchronized sensorimotor and parieto-occipital communication of each hemisphere, with the information flow showing unchanged activity patterns when volitionally modulating either the dominant or the non-dominant hemisphere. This observed topography of information flow might serve different purposes. On the one hand, the interconnection of sensory regions with parietal regions is important for sensorimotor integration, providing as it does information about the current state of the hand, while the sensory feedback comprises feed-forward information that is important for motor learning [Gandolla et al., 2014; Hardwick et al., 2013]. On the other hand, the motor-parietal connection might be related to greater visuomotor integration, where higher states of coupling are possibly linked to a greater capacity for visuomotor integration [Karabanov et al., 2012; Wu et al., 2014; Beuter and Modolo, 2009; Feurra et al., 2011; Ma et al., 2011]. Moreover, information flow from motor regions might have a top-down-related predictive influence of sensory consequences upon somatosensory and parietal regions [Gandolla et al., 2014] by matching haptic/proprioceptive feedback and volitional control. Such a modular representation of hand and finger gestures are known to exist in the circuitry of the motor cortex [Krakauer and Mazzoni, 2011].

There are several possible explanations for the bihemispheric activation between sensorimotor and parieto-occipital regions shown by LH. One possibility is that LH and RH have different anatomical connectivity patterns [Galaburda et al., 1978; Witelson, 1985]. Moreover, LH show less functional asymmetries of interhemispheric inhibition or facilitation between homologous sensorimotor regions [De Gennaro et al., 2004; Brouwer et al., 2001; Bernard et al., 2011; Civardi et al., 2000; Netz et al., 1995; Reid and Serrien, 2014]. Moreover, LH generally use their non-dominant (right) hand to adapt to a preferentially right-handed world. The original hand dominance is modified by an environmental factor, such that LH might not be able to fully express their hand dominance and therefore do not lateralize as extensively as RH [Willems et al., 2014]. However, this study revealed that, regardless of handedness, the large-scale oscillatory signatures for self-regulation of brain activity remained unaffected by hemispheric specialization. Even though we did not detect gender-specific effects, future studies will need to evaluate this question in greater detail also [Cantillo-Negrete et al., 2014].

Albeit acquired in healthy subjects, the findings presented here may inform interventions in stroke survivors with different treatment outcomes due to their respective hand dominance [Harris and Eng, 2006; Langan and van Donkelaar, 2008; McCombe Waller and Whittall, 2005; Rinehart et al., 2009]. The findings of this study suggest that inherent characteristics such as hemispheric specialization and handedness do not limit the application of this neurofeedback approach for patient

populations. When the  $\beta$ -modulation range is compromised after stroke right- and left-handers may, however, utilize different cortical  $\alpha$ -networks for compensation and/or relearning. Addressing these neurophysiological substrates of volitional modulation of oscillatory activity more specifically may enable us to develop these neurofeedback approaches into more effective tools for neurorehabilitation and functional restoration.

When designing interventions based on brain self-regulation, individual  $\alpha$ -band networks could thus serve as more specific neuronal substrates for volitional modulation than the regional sensorimotor rhythms that are presently in use. Moreover, these neurophysiological profiles might provide the target for even more individualized rehabilitation approaches, addressing the described network dynamics with additional state-dependent interventions such as neuromodulation [Naros and Gharabaghi, 2017; Kraus et al., 2016b, 2018; Gharabaghi et al., 2014].

## 5. Conclusion

In healthy subjects, sensorimotor  $\beta$ -band activity can be robustly modulated by motor imagery and proprioceptive feedback in both hemispheres independent of handedness. However, right and left handers show different oscillatory entrainment of cortical alpha-band networks during neurofeedback. This finding may inform neurofeedback interventions in future to align them more precisely with the underlying physiology.

## Data availability statement

The dataset is available for qualified researchers upon reasonable request.

## Data code statement

All data analysis was performed offline with scripts in MATLAB<sup>®</sup> and available codes from open source toolboxes that are referenced in the paper.

## Conflicts of interest

The authors report no conflict of interest.

## Acknowledgements and funding

This work was supported by the Baden-Wuerttemberg Foundation [NEU005, NemoPlast]. MV, RG and VR were supported by the Graduate Training Centre of Neuroscience & International Max Planck Research School, and Graduate School of Neural and Behavioral Sciences, Tuebingen, Germany. MV is currently working at the Institute of Human Factors and Technology Management IAT, University of Stuttgart, Germany, and the Fraunhofer Institute for Industrial Engineering IAO, Stuttgart, Germany. PB is currently working at the Department of Neurology & Stroke/Hertie Institute for Clinical Brain Research (University of Tuebingen). AG is supported by the German Federal Ministry of Education and Research [BMBF 13GW0119B, IMONAS; 13GW0214B, INSPIRATION; 13GW0270B, INAUDITAS]. We thank Christoph Braun and Kevin Kern for helpful comments on the manuscript. Furthermore, we thank Sudarshan Sekhar for technical support during the measurements.

## References

Averbeck, B.B., Battaglia-Mayer, A., Guglielmo, C., Caminiti, R., 2009. Statistical analysis of parieto-frontal cognitive-motor networks. *J. Neurophysiol.* 102, 1911–1920.

Babiloni, F., Cincotti, F., Babiloni, C., Carducci, F., Mattia, D., Astolfi, L., Basilisco, A., Rossini, P.M., Ding, L., Ni, Y., Cheng, J., Christine, K., Sweeney, J., He, B., 2005. Estimation of the cortical functional connectivity with the multimodal integration of

high-resolution EEG and fMRI data by directed transfer function. *Neuroimage* 24, 118–131.

Baker, S.N., Pinches, E.M., Lemon, R.N., 2003. Synchronization in monkey motor cortex during a precision grip task. II. effect of oscillatory activity on corticospinal output. *J. Neurophysiol.* 89, 1941–1953.

Bauer, R., Fels, M., Vukelić, M., Ziemann, U., Gharabaghi, A., 2015. Bridging the gap between motor imagery and motor execution with a brain-robot interface. *Neuroimage* 108, 319–327, 2015 Mar.

Bauer, R., Gharabaghi, A., 2015a. Reinforcement learning for adaptive threshold control of restorative brain-computer interfaces: a Bayesian simulation. *Front. Neurosci.* 9, 36.

Bauer, R., Gharabaghi, A., 2015b. Estimating cognitive load during self-regulation of brain activity and neurofeedback with therapeutic brain-computer interfaces. *Front. Behav. Neurosci.* 9, 21.

Bauer, R., Fels, M., Royter, V., Raco, V., Gharabaghi, A., 2016a. Closed-loop adaptation of neurofeedback based on mental effort facilitates reinforcement learning of brain self-regulation. *Clin. Neurophysiol.* 127, 3156–3164.

Bauer, R., Vukelić, M., Gharabaghi, A., 2016b. What is the optimal task difficulty for reinforcement learning of brain self-regulation? *Clin. Neurophysiol.* 127, 3033–3041.

Bauer, R., Gharabaghi, A., 2017. Constraints and adaptation of closed-loop neuroprosthetics for functional restoration. *Front. Neurosci.* 11, 111.

Belardinelli, P., Laer, L., Ortiz, E., Braun, C., Gharabaghi, A., 2017. Plasticity of premotor cortico-muscular coherence in severely impaired stroke patients with hand paralysis. *NeuroImage. Clin.* 14, 726–733.

Benjamini, Y., Hochberg, Y., 1995. Controlling the false discovery rate: a practical and powerful approach to multiple testing. *J. R. Stat. Soc. Ser. B Methodol.* 57, 289–300.

Bernard, J.A., Taylor, S.F., Seidler, R.D., 2011. Handedness, dexterity, and motor cortical representations. *J. Neurophysiol.* 105, 88–99.

Beuter, A., Modolo, J., 2009. Delayed and lasting effects of deep brain stimulation on locomotion in Parkinson's disease. *Chaos* 19, 026114.

Blankertz, B., Sannelli, C., Halder, S., Hammer, E.M., Kübler, A., Müller, K.-R., Curio, G., Dichgans, T., 2010. Neurophysiological Predictor of SMR-Based BCI Performance. *NeuroImage*, vol. 51, pp. 1303–1309.

Bollimunta, A., Chen, Y., Schroeder, C.E., Ding, M., 2008. Neuronal mechanisms of cortical alpha oscillations in awake-behaving macaques. *J. Neurosci.* 28, 9976–9988.

Brauchle, D., Vukelić, M., Bauer, R., Gharabaghi, A., 2015. Brain state-dependent robotic reaching movement with a multi-joint arm exoskeleton. Combining brain-machine interfacing and robotic rehabilitation. *Front. Hum. Neurosci.* 9, 564.

Brouwer, B., Sale, M.V., Nordstrom, M.A., 2001. Asymmetry of motor cortex excitability during a simple motor task: relationships with handedness and manual performance. *Exp. Brain Res.* 138, 467–476.

Buccino, G., Binkofski, F., Fink, G.R., Fadiga, L., Fogassi, L., Gallese, V., Seitz, R.J., Zilles, K., Rizzolatti, G., Freund, H.J., 2001. Action observation activates premotor and parietal areas in a somatotopic manner: an fMRI study. *Eur. J. Neurosci.* 13, 400–404.

Burianová, H., Marstaller, L., Sowman, P., Tesan, G., Rich, A.N., Williams, M., Johnson, B.W., 2013. Multimodal functional imaging of motor imagery using a novel paradigm. *Neuroimage* 71, 50–58.

Cantillo-Negrete, J., Gutierrez-Martinez, J., Carino-Escobar, R.I., Carrillo-Mora, P., Elias-Vinas, D., 2014 Dec 4. An approach to improve the performance of subject-independent BCIs-based on motor imagery allocating subjects by gender. *Biomed. Eng. Online* 13, 158.

Capotosto, P., Babiloni, C., Romani, G.L., Corbetta, M., 2009. Frontoparietal cortex controls spatial attention through modulation of anticipatory alpha rhythms. *J. Neurosci.* 29, 5863–5872.

Christensen, M.S., Lundbye-Jensen, J., Geertsen, S.S., Petersen, T.H., Paulson, O.B., Nielsen, J.B., 2007. Premotor cortex modulates somatosensory cortex during voluntary movements without proprioceptive feedback. *Nat. Neurosci.* 10, 417–419.

Civardi, C., Cavalli, A., Naldi, P., Varrasi, C., Cantello, R., 2000. Hemispheric asymmetries of cortico-cortical connections in human hand motor areas. *Clin. Neurophysiol.* 111, 624–629.

Darvishi, S., Gharabaghi, A., Boulay, C.B., Ridding, M.C., Abbott, D., Baumert, M., 2017. Proprioceptive feedback facilitates motor imagery-related operant learning of sensorimotor  $\beta$ -band modulation. *Front. Neurosci.* 11, 60, 2017.

De Gennaro, L., Cristiani, R., Bertini, M., Curcio, G., Ferrara, M., Fratello, F., Romei, V., Rossini, P.M., 2004. Handedness is mainly associated with an asymmetry of corticospinal excitability and not of transcallosal inhibition. *Clin. Neurophysiol.* 115, 1305–1312.

De Nooijer, J.A., van Gog, T., Paas, F., Zwaan, R.A., 2013. When left is not right: handedness effects on learning object-manipulation words using pictures with left- or right-handed first-person perspectives. *Psychol. Sci.* 24, 2515–2521.

Delorme, A., Makeig, S., 2004. EEGLAB: an open source toolbox for analysis of single-trial EEG dynamics including independent component analysis. *J. Neurosci. Methods* 134, 9–21.

Dobkin, B.M., 2004. Strategies for stroke rehabilitation. *Lancet Neurol.* 3, 528–536.

Eliassen, J.C., Baynes, K., Gazzaniga, M.S., 2000. Anterior and posterior callosal contributions to simultaneous bimanual movements of the hands and fingers. *Brain J. Neurol.* 123, 2501–2511. Pt 12.

Ewald, A., Marzetti, L., Zappasodi, F., Meinecke, F.C., Nolte, G., 2012. Estimating True Brain Connectivity from EEG/MEG Data Invariant to Linear and Static Transformations in Sensor Space. *NeuroImage*, vol. 60, pp. 476–488.

Fels, M., Bauer, R., Gharabaghi, A., 2015. Predicting workload profiles of brain-robot interface and electromyographic neurofeedback with cortical resting-state networks: personal trait or task-specific challenge? *J. Neural Eng.* 12 (4), 046029.

Feurra, M., Bianco, G., Polizzotto, N.R., Innocenti, I., Rossi, A., Rossi, S., 2011. Cortico-cortical connectivity between right parietal and bilateral primary motor cortices

- during imagined and observed actions: a combined TMS/tcds study. *Front. Neural Circuits* 10.
- Galaburda, A.M., LeMay, M., Kemper, T.L., Geschwind, N., 1978. Right-left Asymmetries in the Brain Science, vol.199, pp. 852–856.
- Gandolla, M., Ferrante, S., Molteni, F., Guanziroli, E., Frattini, T., Martegani, A., Ferrigno, G., Friston, K., Pedrocchi, A., Ward, N.S., 2014. Re-thinking the role of motor cortex: context-sensitive motor outputs? *Neuroimage* 91C, 366–374.
- Gao, Q., Duan, X., Chen, H., 2011. Evaluation of Effective Connectivity of Motor Areas during Motor Imagery and Execution Using Conditional Granger Causality *NeuroImage*, vol. 54, 1280–8.
- Gharabaghi, A., Kraus, D., Leão, M.T., Spüler, M., Walter, A., Bogdan, M., Rosenstiel, W., Naros, G., Ziemann, U., 2014. Coupling brain-machine interfaces with cortical stimulation for brain-state dependent stimulation: enhancing motor cortex excitability for neurorehabilitation. *Front. Hum. Neurosci.* 8, 122.
- Gharabaghi, A., 2016. What turns assistive into restorative brain-machine interfaces? *Front. Neurosci.* 10, 456.
- Gomez-Rodriguez, M., Peters, J., Hill, J., Schölkopf, B., Gharabaghi, A., Grosse-Wentrup, M., 2011. Closing the sensorimotor loop: haptic feedback facilitates decoding of motor imagery. *J. Neural Eng.* 8, 036005.
- Gonzalez, C.L.R., Ganel, T., Whitwell, R.L., Morrissey, B., Goodale, M.A., 2008. Practice Makes Perfect, but Only with the Right Hand: Sensitivity to Perceptual Illusions with Awkward Grasps Decreases with Practice in the Right but Not the Left Hand *Neuropsychologia*, vol. 46, pp. 624–631.
- Graziano, M.S.A., Taylor, C.S.R., Moore, T., 2002a. Complex Movements Evoked by Microstimulation of Precentral Cortex Neuron, vol. 34, pp. 841–851.
- Graziano, M.S.A., Taylor, C.S.R., Moore, T., Cooke, D.F., 2002b. The Cortical Control of Movement Revisited *Neuron*, vol. 36, pp. 349–362.
- Haegens, S., Nàcher, V., Luna, R., Romo, R., Jensen, O., 2011.  $\alpha$ -Oscillations in the monkey sensorimotor network influence discrimination performance by rhythmic inhibition of neuronal spiking. *Proc. Natl. Acad. Sci. U. S. A.* 108, 19377–19382.
- Halder, S., Agorastos, D., Veit, R., Hammer, E.M., Lee, S., Varkuti, B., Bogdan, M., Rosenstiel, W., Birbaumer, N., Kübler, A., 2011. Neural Mechanisms of Brain–Computer Interface Control *NeuroImage*, vol. 55, pp. 1779–1790.
- Halsband, U., Lange, R.K., 2006. Motor learning in man: a review of functional and clinical studies. *J. Physiol. Paris* 99, 414–424.
- Hardwick, R.M., Rottschy, C., Miall, R.C., Eickhoff, S.B., 2013. A Quantitative Meta-Analysis and Review of Motor Learning in the Human Brain *NeuroImage*, vol.67, pp. 283–297.
- Harris, J.E., Eng, J.J., 2006. Individuals with the dominant hand affected following stroke demonstrate less impairment than those with the nondominant hand affected. *Neurorehabil. Neural Repair* 20, 380–9.
- Haufe, S., Nikulin, V.V., Müller, K.-R., Nolte, G., 2013. A Critical Assessment of Connectivity Measures for EEG Data: a Simulation Study *NeuroImage*, vol. 64, pp. 120–133.
- Heinrichs-Graham, E., Arpin, D.J., Wilson, T.W., 2016. Cue-related temporal factors modulate movement-related beta oscillatory activity in the human motor circuit. *J. Cogn. Neurosci.* 28 (7), 1039–1051.
- Ionta, S., Blanke, O., 2009. Differential influence of hands posture on mental rotation of hands and feet in left and right handers. *Exp. Brain Res.* 195, 207–217.
- Ionta, S., Fourkas, A.D., Fiorio, M., Aglioti, S.M., 2007. The influence of hands posture on mental rotation of hands and feet *Exp. Brain Res.* 183, 1–7.
- Jackson, A., Spinks, R.L., Freeman, T.C.B., Wolpert, D.M., Lemon, R.N., 2002. Rhythm generation in monkey motor cortex explored using pyramidal tract stimulation. *J. Physiol.* 541, 685–699.
- Jeannerod, M., 2001. Neural Simulation of Action: a Unifying Mechanism for Motor Cognition *NeuroImage*, vol. 14, S103–9.
- Jensen, O., Mazaheri, A., 2010. Shaping functional architecture by oscillatory alpha activity: gating by inhibition *Front. Hum. Neurosci.* 4, 186.
- Kamiński, M., Ding, M., Truccolo, W.A., Bressler, S.L., 2001. Evaluating causal relations in neural systems: granger causality, directed transfer function and statistical assessment of significance. *Biol. Cybern.* 85, 145–157.
- Karabanov, A., Jin, S.-H., Joutsen, A., Poston, B., Aizen, J., Ellenstein, A., Hallett, M., 2012. Timing-dependent modulation of the posterior parietal cortex-primary motor cortex pathway by sensorimotor training. *J. Neurophysiol.* 107, 3190–3199.
- Khademi, F., Royter, V., Gharabaghi, A., 2018. Distinct beta-band oscillatory circuits underlie corticospinal gain modulation. *Cerebr. Cortex* 28 (4), 1502–1515.
- Kilavik, B.E., Zaepffel, M., Brovelli, A., MacKay, W.A., Riehle, A., 2013. The ups and downs of  $\beta$  oscillations in sensorimotor cortex. *Exp. Neurol.* 245, 15–26.
- Klimesch, W., 2012. Alpha-band oscillations, attention, and controlled access to stored information *Trends. Cogn. Sci.* 16, 606–617.
- Koch, G., Fernandez Del Olmo, M., Cheeran, B., Ruge, D., Schippling, S., Caltagirone, C., Rothwell, J.C., 2007. Focal stimulation of the posterior parietal cortex increases the excitability of the ipsilateral motor cortex. *J. Neurosci. Off. J. Soc. Neurosci.* 27, 6815–6822.
- Krakauer, J.W., Mazzoni, P., 2011. Human sensorimotor learning: adaptation, skill, and beyond. *Curr. Opin. Neurobiol.* 21, 636–644.
- Kraus, D., Gharabaghi, A., 2015. Projecting navigated TMS sites on the gyral anatomy decreases inter-subject variability of cortical motor maps. *Brain Stimul* 8, 831–837.
- Kraus, D., Gharabaghi, A., 2016. Neuromuscular plasticity. Disentangling stable and variable motor maps in the human sensorimotor cortex. *Neural Plast.* <https://doi.org/10.1155/2016/7365609>, 7365609.
- Kraus, D., Naros, G., Bauer, R., Leão, M.T., Ziemann, U., Gharabaghi, A., 2016a. Brain-robot interface driven plasticity. Distributed modulation of corticospinal excitability. *Neuroimage* 125, 522–532.
- Kraus, D., Naros, G., Bauer, R., Khademi, F., Leão, M.T., Ziemann, U., Gharabaghi, A., 2016b. Brain state-dependent transcranial magnetic closed-loop stimulation controlled by sensorimotor desynchronization induces robust increase of corticospinal excitability. *Brain Stimul* 9, 415–424.
- Kraus, D., Naros, G., Guggenberger, R., Leão, M.T., Ziemann, U., Gharabaghi, A., 2018. Recruitment of additional corticospinal pathways in the human brain with state-dependent paired associative stimulation. *J. Neurosci.* 38, 1396–1407.
- Lalazar, H., Vaadia, E., 2008. Neural basis of sensorimotor learning: modifying internal models. *Curr. Opin. Neurobiol.* 18, 573–581.
- Langan, J., van Donkelaar, P., 2008. The influence of hand dominance on the response to a constraint-induced therapy program following stroke *Neurorehabil. Neural Repair* 22, 298–304.
- Ma, L., Narayana, S., Robin, D.A., Fox, P.T., Xiong, J., 2011. Changes Occur in Resting State Network of Motor System during 4 Weeks of Motor Skill Learning *NeuroImage*, vol. 58, pp. 226–233.
- Malouin, F., Richards, C.L., Jackson, P.L., Lafleur, M.F., Durand, A., Doyon, J., 2007. The Kinesthetic and Visual Imagery Questionnaire (KVIQ) for assessing motor imagery in persons with physical disabilities: a reliability and construct validity study. *J. Neurol. Phys. Ther.* 31, 20–29.
- Mathew, J., Kübler, A., Bauer, R., Gharabaghi, A., 2016. Probing corticospinal recruitment patterns and functional synergies with transcranial magnetic stimulation. *Front. Cell. Neurosci.* 10, 175.
- McCombe Waller, S., Whittall, J., 2005. Hand dominance and side of stroke affect rehabilitation in chronic stroke *Clin. Rehabil.* 19, 544–551.
- McFarland, D.J., Wolpaw, J.R., 2008. Sensorimotor rhythm-based brain-computer interface (BCI): model order selection for autoregressive spectral analysis. *J. Neural Eng.* 5, 155–162.
- McFarland, D.J., Miner, L.A., Vaughan, T.M., Wolpaw, J.R., 2000. Mu and Beta Rhythm Topographies during Motor Imagery and Actual Movements *Brain Topogr.* vol. 12, pp. 177–186.
- Miller, K.J., Schalk, G., Fetz, E.E., den Nijs, M., Ojemann, J.G., Rao, R.P.N., 2010. Cortical activity during motor execution, motor imagery, and imagery-based online feedback. *Proc. Natl. Acad. Sci. U. S. A.* 107, 4430–4435.
- Mo, J., Schroeder, C.E., Ding, M., 2011. Attentional modulation of alpha oscillations in macaque inferotemporal cortex. *J. Neurosci. Off. J. Soc. Neurosci.* 31, 878–882.
- Muthukumaraswamy, S.D., Myers, J.F.M., Wilson, S.J., Nutt, D.J., Lingford-Hughes, A., Singh, K.D., et al., 2013. The effects of elevated endogenous GABA levels on movement-related network oscillations. *Neuroimage* 66, 36–41.
- Naros, G., Gharabaghi, A., 2015. Reinforcement learning of self-regulated  $\beta$ -oscillations for motor restoration in chronic stroke. *Front. Hum. Neurosci.* 9, 391.
- Naros, G., Naros, I., Grimm, F., Ziemann, U., Gharabaghi, A., 2016. Reinforcement learning of self-regulated sensorimotor  $\beta$ -oscillations improves motor performance. *Neuroimage* 134, 142–152.
- Naros, G., Gharabaghi, 2017. A Physiological and behavioral effects of  $\beta$ -TACS on brain self-regulation in chronic stroke. *Brain Stimul* 10, 251–259.
- Netz, J., Ziemann, U., Hömberg, V., 1995. Hemispheric asymmetry of transcallosal inhibition in man *Exp. Brain Res. Exp. Hirnforsch. Experiment. Cérébrale* 104, 527–533.
- Neuper, C., Scherer, R., Reiner, M., Pfurtscheller, G., 2005. Imagery of motor actions: differential effects of kinesthetic and visual–motor mode of imagery in single-trial EEG. *Cogn. Brain Res.* 25, 668–677.
- Nolte, G., Bai, O., Wheaton, L., Mari, Z., Vorbach, S., Hallett, M., 2004. Identifying true brain interaction from EEG data using the imaginary part of coherency. *Clin. Neurophysiol. Off. J. Int. Fed. Clin. Neurophysiol.* 115, 2292–2307.
- Nolte, G., Ziehe, A., Nikulin, V.V., Schlögl, A., Krämer, N., Brismar, T., Müller, K.-R., 2008. Robustly estimating the flow direction of information in complex physical systems. *Phys. Rev. Lett.* 100, 234101.
- Oldfield, R.C., 1971. The Assessment and Analysis of Handedness: the Edinburgh Inventory *Neuropsychologia*, vol. 9, pp. 97–113.
- Palva, S., Palva, J.M., 2011. Functional roles of alpha-band phase synchronization in local and large-scale cortical networks. *Front. Psychol.* 2, 204.
- Palva, S., Kulashekhar, S., Hämäläinen, M., Palva, J.M., 2011. Localization of cortical phase and amplitude dynamics during visual working memory encoding and retention. *J. Neurosci. Off. J. Soc. Neurosci.* 31, 5013–5025.
- Pfurtscheller, G., Lopes da Silva, F.H., 1999. Event-related EEG/MEG synchronization and desynchronization. *Clin. Neurophysiol. Off. J. Int. Fed. Clin. Neurophysiol.* 110, 1842–1857.
- Pfurtscheller, G., Solis-Escalante, T., 2009. Could the beta rebound in the EEG be suitable to realize a “brain switch”? *Clin. Neurophysiol. Off. J. Int. Fed. Clin. Neurophysiol.* 120, 24–29.
- Pineda, J.A., 2005. The functional significance of mu rhythms: translating “seeing” and “hearing” into “doing”. *Brain Res. Brain Res. Rev.* 50, 57–68.
- Reid, C.S., Serrien, D.J., 2014. Primary Motor Cortex and Ipsilateral Control: a TMS Study *Neuroscience*, vol. 270, 20–6.
- Rinehart, J.K., Singleton, R.D., Adair, J.C., Sadek, J.R., Haaland, K.Y., 2009. Arm use after left or right hemiparesis is influenced by hand preference *Stroke. J. Cereb. Circ.* 40, 545–550.
- Romei, V., Thut, G., Silvanto, J., 2016. Information-based approaches of noninvasive transcranial brain stimulation. *Trends Neurosci.* 39 (11), 782–795.
- Rossiter, H.E., Boudrias, M.-H., Ward, N.S., 2014a. Do movement-related beta oscillations change following stroke? *J. Neurophysiol.* 112 (9), 2053–2058.
- Rossiter, H.E., Davis, E.M., Clark, E.V., Boudrias, M.H., Ward, N.S., 2014b. Beta oscillations reflect changes in motor cortex inhibition in healthy ageing. *Neuroimage* 91, 360–365.
- Royter, V., Gharabaghi, A., 2016. Brain state-dependent closed-loop modulation of paired associative stimulation controlled by sensorimotor desynchronization. *Front. Cell. Neurosci.* 10, 115.

- Sanei, S., 2007. EEG Signal Processing. John Wiley & Sons, Chichester, England ; Hoboken, NJ.
- Schalk, G., McFarland, D.J., Hinterberger, T., Birbaumer, N., Wolpaw, J.R., 2004. BCI2000: a general-purpose brain-computer interface (BCI) system. *IEEE Trans. Biomed. Eng.* 51, 1034–1043.
- Schubotz, R.I., von Cramon, D.Y., 2003. Functional-anatomical concepts of human premotor cortex: evidence from fMRI and PET studies. *Neuroimage* 20 (Suppl. 1), S120–S131.
- Shadmehr, R., Holcomb, H.H., 1997. Neural Correlates of Motor Memory Consolidation. *Science*, vol. 277, 821–5.
- Shiner, C., Tang, H., Johnson, B., McNulty, P., 2015. Cortical beta oscillations and motor thresholds differ across the spectrum of post-stroke motor impairment, a preliminary MEG and TMS study. *Brain Res.* 1629, 26–37.
- Smith, M.E., Gevins, A., Brown, H., Karnik, A., Du, R., 2001. Monitoring task loading with multivariate EEG measures during complex forms of human-computer interaction. *Hum. Factors J. Hum. Factors Ergon. Soc* 43, 366–380.
- Smith, M.E., McEvoy, L.K., Gevins, A., 1999. Neurophysiological indices of strategy development and skill acquisition. *Brain Res. Cogn. Brain Res* 7, 389–404.
- Solis-Escalante, T., Müller-Putz, G.R., Pfurtscheller, G., Neuper, C., 2012. Cue-induced beta rebound during withholding of overt and covert foot movement. *Clin. Neurophysiol. Off. J. Int. Fed. Clin. Neurophysiol* 123, 1182–1190.
- Suminski, A.J., Tkach, D.C., Fagg, A.H., Hatsopoulos, N.G., 2010. Incorporating feedback from multiple sensory modalities enhances brain-machine interface control. *J. Neurosci. Off. J. Soc. Neurosci* 30, 16777–16787.
- Suzuki, W.A., 2007. Integrating Associative Learning Signals across the Brain Hippocampus, vol. 17, pp. 842–850.
- Szameitat, A.J., Shen, S., Conforto, A., Sterr, A., 2012. Cortical Activation during Executed, Imagined, Observed, and Passive Wrist Movements in Healthy Volunteers and Stroke Patients *NeuroImage*, vol. 62, pp. 266–280.
- Vahdat, S., Darainy, M., Milner, T.E., Ostry, D.J., 2011. Functionally specific changes in resting-state sensorimotor networks after motor learning. *J. Neurosci. Off. J. Soc. Neurosci* 31, 16907–15.
- Vukelić, M., Bauer, R., Naros, G., Naros, I., Braun, C., Gharabaghi, A., 2014. Lateralized Alpha-Band Cortical Networks Regulate Volitional Modulation of Beta-Band Sensorimotor Oscillations *NeuroImage*, vol. 87, pp. 147–153.
- Vukelić, M., Gharabaghi, A., 2015a. Oscillatory entrainment of the motor cortical network during motor imagery is modulated by the feedback modality. *Neuroimage* 111, 1–11.
- Vukelić, M., Gharabaghi, A., 2015b. Self-regulation of circumscribed brain activity modulates spatially selective and frequency specific connectivity of distributed resting state networks. *Front. Behav. Neurosci.* 9, 181.
- Wander, J.D., Blakely, T., Miller, K.J., Weaver, K.E., Johnson, L.A., Olson, J.D., Fetz, E.E., Rao, R.P.N., Ojemann, J.G., 2013. Distributed cortical adaptation during learning of a brain-computer interface task. *Proc. Natl. Acad. Sci. U. S. A* 110, 10818–10823.
- Weisz, N., Wühle, A., Monitola, G., Demarchi, G., Frey, J., Popov, T., Braun, C., 2014. Prestimulus oscillatory power and connectivity patterns predispose conscious somatosensory perception. *Proc. Natl. Acad. Sci. Unit. States Am.* 111, E417–E425.
- Willems, R.M., der Haegen, L.V., Fisher, S.E., Francks, C., 2014. On the other hand: including left-handers in cognitive neuroscience and neurogenetics. *Nat. Rev. Neurosci.* 15, 193–201.
- Witelson, S.F., 1985. The Brain Connection: the Corpus Callosum Is Larger in Left-Handers *Science*, vol. 229, 665–8.
- Wu, J., Srinivasan, R., Kaur, A., Cramer, S.C., 2014. Resting-state Cortical Connectivity Predicts Motor Skill Acquisition *NeuroImage*, 91C, pp. 84–90.